IARJSET ISSN (O) 2393-8021, ISSN (P) 2394-1588

International Advanced Research Journal in Science, Engineering and Technology

ISO 3297:2007 Certified ⁜ Impact Factor 7.105 ⁜ Vol. 9, Issue 5, May 2022

DOI: 10.17148/IARJSET.2022.9591

Seismic Response of Torsionally Coupled Building Isolated with Multiple-Variable Frequency Pendulum Isolator

Jay Hodar[1], Vishal Patel[2], Atul Desai[3]

M.Tech, Structural Engineering, Birla Vishvakarma Mahavidyalaya, Vallabh Vidhyanagar, India[1]

Assistant Professor, Structural Engineering, Birla Vishvakarma Mahavidyalaya, Vallabh Vidhyanagar, India[2]

Professor and Head, Structural Engineering, Birla Vishvakarma Mahavidyalaya, Vallabh Vidhyanagar, India[3]

Abstract: The behaviour of torsionally coupled structures isolated using a Multiple-variable frequency pendulum system (MVFPI) is discussed (Recently developed advanced friction base isolator). Because of the constant isolator period and restoring force features of the friction pendulum system (FPS), this MVFPI overcomes these restrictions. Most presently available methods, such as the friction pendulum system (FPS) and the pure friction (PF) system, however, have practical limits and are ineffective when the input excitation level differs greatly from the design level. A novel technology dubbed the multiple variable frequency pendulum isolator (MVFPI) has been designed to address these constraints while maintaining the benefits. To integrate the seismic performance of MVFPI with varied seismic intensities, the sliding surface of MVFPI was specified as a continuous piecewise function. Newmark's step-by-step technique is used to construct and solve the governing equations of motion of the building-isolation system, assuming linear acceleration change over tiny time intervals. In this research, six pairs of near-fault ground movements are used as input ground motions. The response ratio between the peak responses of the torsionally linked structure with and without the MVFPI is used to measure the efficiency of the base isolation utilizing the MVFPI. For chosen earthquake ground movements, the coupled lateral-torsional response is calculated using various parameter modifications. Furthermore, a parametric investigation of MVFPI-isolated structures was compared to FPS. The parametric study's numerical findings aid in understanding the torsional behavior of the MVFPI-isolated structure. The MVFPI is proven to perform much better than the FPS in terms of reducing base shear and torque responses. Also square model has been compared with rectangle model for different parameters.

Keywords: Multiple-variable frequency pendulum system, base isolation, near-fault ground motion, asymmetric building, eccentricity ratio, the torsional coupling, uncoupled time period.

I. INTRODUCTION

Base isolation is considered as an effective technique for aseismic design of structures. A flexible layer (or isolator) is placed between the structure and its foundation in base isolation, allowing relative deformations at this level. Because the isolator is flexible, its time period of motion is longer than that of the structure, and the isolator time period influences the isolated structure's fundamental period [7]. The isolator time period is substantially longer for correctly constructed isolation systems than for those containing significant ground motion energy. As a result, the employment of an isolator shifts the structure's basic period away from dominating times of ground excitation, lowering the amount of energy delivered into the structure. Because of the asymmetric nature of torsionally connected structures, their seismic reaction is severe. The typical way of making them earthquake-resistant involves increasing the structure's strength and energy-absorbing capacity. Inelastic deformation, on the other hand, has caused structural and non-structural damage to many constructions. To protect sensitive instruments, an alternate approach known as base isolation is frequently utilized today for earthquake-resistant structural systems design. A base isolation system's fundamental premise is to isolate the structure from the ground by utilizing isolators between the structure's base and foundation. Two fundamental qualities of these base isolators are (1) horizontal flexibility and energy-absorbing capability. The isolator's horizontal flexibility lowers the structure's fundamental frequency below the frequency range that dominates in ordinary earthquake excitation, and (2) its energy-absorbing capability reduces both relative displacements and seismic energy delivered to the structure.

Several sliding base isolation systems have been invented and explored in the past, including the friction pendulum system (FPS) [1], the variable frequency pendulum isolator (VFPI) [2], the double concave friction pendulum (DCFP) bearing [3], and the triple friction pendulum bearing [4]. The FPS is the most appealing of the numerous friction base isolators because of its ease of installation and simple process of restoring force using gravity. This isolator combines the sliding and recentering mechanics into a single component. Because FPS's sliding surface is spherical, the basic

IARJSET ISSN (O) 2393-8021, ISSN (P) 2394-1588

International Advanced Research Journal in Science, Engineering and Technology

ISO 3297:2007 Certified ⁜ Impact Factor 7.105 ⁜ Vol. 9, Issue 5, May 2022

DOI: 10.17148/IARJSET.2022.9591

oscillation period remains constant. Through friction, the FPS can give as much as 50% comparable dampening. The FPS intended for a specific excitation intensity, on the other hand, may not operate well during earthquakes of substantially higher intensity [5]. The Variable Frequency Pendulum Isolator (VFPI) was proposed by certain researchers [6-8] based on the FPS to lessen the excessive seismic response generated by earthquakes with a large long-period wave. The geometry of the sliding surface is predefined by a continuous function, which distinguishes VFPI from FPS. As a result, when VFPI is subjected to near-fault ground vibrations, the VFPI isolated structure's natural frequency is moved away from the prevailing frequency. To circumvent the FPS limits, a multiple-variable frequency pendulum isolator (MVFPI) was created. To integrate the seismic performance of MVFPI with varied seismic intensities, the sliding surface of the MVFPI was predefined as a continuous piecewise function. To improve durability and regulate deformation, high-performance materials such as polytetrafluoroethylene (PTFE) fabric and shape memory alloy (SMA) were used [9].

Despite the immediate benefits of seismic base isolation technology, some experts believe that base-isolated structures are vulnerable to significant pulse like ground vibrations caused near fault zones. [10]. Near-fault ground motions can differ significantly from far-fault ground motions. Because no attempt has been made on the MVFPI isolator, investigation of torsionally coupled structure isolated with MVFPI subjected to bi-directional near-fault ground motions is required. In addition, FPS will be used in a comparison study. A response study of torsionally coupled one-story buildings isolated using MVFPI is described in this paper. Newmark's step-by-step procedure is used to acquire the responses. The study's main goals are to: (1) explore the seismic response of torsionally linked buildings isolated with MVFPI. (2) To compare a building isolated with a Multiple-variable frequency pendulum isolator (MVFPI) and one isolated with a Friction pendulum system (FPS). (3) To conduct a parametric study of the torsionally coupled building isolated with MVFPI in terms of seismic response. (4) To compare a building isolated with a Multiple-variable frequency pendulum isolator (MVFPI) for square and rectangle model

II. DESCRIPTION OF MVFPI

When subjected to ground excitations involving long-period components, such as near fault ground motion [9], FPS invariably introduces a constant dominating period, resulting in resonant-like behaviour. MVFPI [9] was created to overcome these limitations and to minimize the seismic response of the structure under various earthquake intensities.
To obtain optimal seismic performance, the geometry of MVFPI's sliding surface is defined as a piecewise function. As shown in fig. 1(b), in the initial stage, the hyperbolic function is used, which has the property of softening stiffness, to

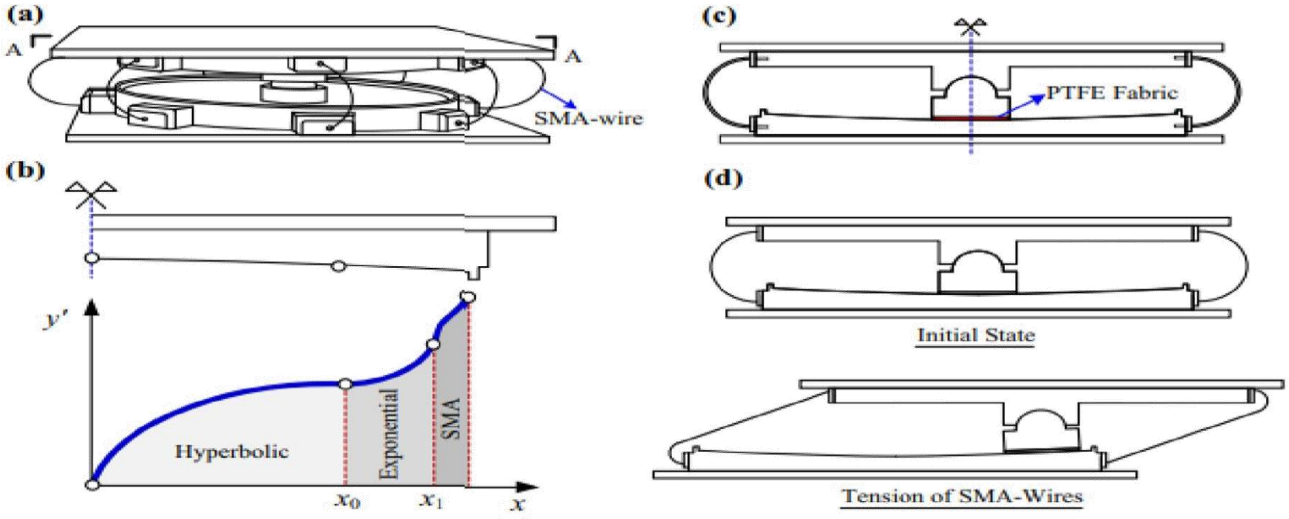

Fig. 1 (a) Configuration of the MVFPI; (b) cross-section of A-A; (c) function of sliding surface; (d) SMA wires in MVFPI.

reduce structural acceleration during an earthquake. However, when the isolator exceeds the critical displacement value x0, the author chooses an exponential function [9], which has the property of enhanced stiffness, to limit the structure's sliding displacement during an earthquake. SMA-wires are placed after the permissible displacement x1 to control deformation and provide the restoring force to improve seismic resilience against earthquakes, as shown in fig. 1. (d). As shown in fig. 1, the MVFPI bearing's sliding surface is made up of polytetrafluoroethylene (PTEF) fabric and highly

IARJSET ISSN (O) 2393-8021, ISSN (P) 2394-1588

International Advanced Research Journal in Science, Engineering and Technology

ISO 3297:2007 Certified ⁜ Impact Factor 7.105 ⁜ Vol. 9, Issue 5, May 2022

DOI: 10.17148/IARJSET.2022.9591

polished stainless steel (c). The PTFE fabric's strong compressive strength and consistent mechanical qualities can help to extend the bearing's life and minimize its size.

III. PROPOSED GEOMETRY OF ISOLATOR

For MVFPI isolator the geometric formula for a sliding surface is given as:

$$y=\begin{cases} b\sqrt{1+\frac{x^2}{(|x|+d)^2}}-b & x \le x_0 \\ y_0 e^{\frac{y'_0}{y_0}(x-x_0)} & x > x_0 \end{cases} \quad (1)$$

Where b is the imaginary semi-axis; d is a constant used to calculate the frequency variation rate; x_0 is the critical displacement between the hyperbolic and exponential functions; y_0 is the function's value at x_0; and y′ is the value of the function's first-order derivative at x_0.

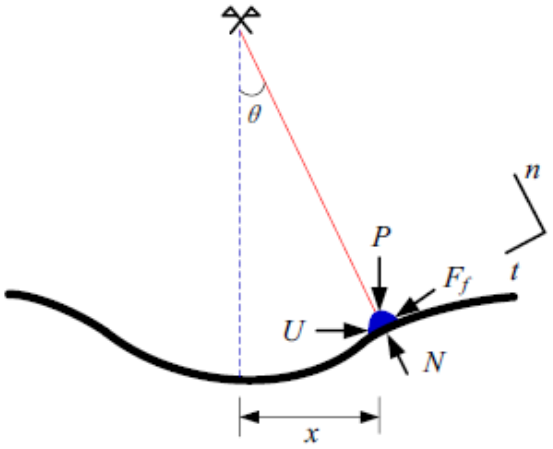

Fig. 2 FBD of slider on the sliding surface

Different Forces acting on the slider are (1) Lateral force *F*, (2) Vertical load *P*, (3) Frictional force F_f, (4) Normal reaction N. now taking equilibrium of forces in horizontal and vertical directions, following relationship are obtained [9]

$$\sum F_n = 0: P\cos\Theta + F\sin\Theta - N = 0 \quad (2)$$

$$\sum F_t = 0: P\sin\Theta - F\cos\Theta + F_f = 0 \quad (3)$$

Combining equations (2) and (3), the force–displacement relationship that governs motion on the sliding surface can be expressed as:

$$F = Py'(x) + \mathrm{sgn}(\dot{x})\mu P\left(\frac{1+y'^2(x)}{1-\mu y'(x)}\right) \quad (4)$$

Where μ is the friction coefficient; sgn(·) is the symbol function.

Assuming that the slope of the sliding surface and friction Coefficient are much smaller than 1 ($y' \ll 1$, $\mu \ll 1$), the above Equation can be simplified as:

$$F = F_r + F_f = Py'(x) + \mathrm{sgn}(\dot{x})\mu P \quad (5)$$

Where the restoring force (*Fr*) and friction force (*Ff*) can be isolated from the horizontal lateral force (*F*). The rate of change of the restoring force (*Fr*) can be used to calculate the equivalent stiffness (*kr*) of the MVFPI bearing:

IARJSET ISSN (O) 2393-8021, ISSN (P) 2394-1588

International Advanced Research Journal in Science, Engineering and Technology

ISO 3297:2007 Certified ⁜ Impact Factor 7.105 ⁜ Vol. 9, Issue 5, May 2022

DOI: 10.17148/IARJSET.2022.9591

$$k_r(x) = \frac{mgy'(x)}{x} \quad (6)$$

Where mg is the superstructure's overall weight. The total isolated structure's oscillation frequency (ω) can be computed by:

$$\omega_b(x) = \sqrt{\frac{g.y'(x)}{x}} \quad (7)$$

Where y′(x) is given by:

$$y'(x) = \frac{\frac{b}{d^2}}{\left(\frac{|x|}{d}+1\right)^2\sqrt{2\left(\frac{x}{d}\right)^2+2\frac{|x|}{d}+1}}\, x \quad (8)$$

As x approaches zero, the initial frequency is:

$$\omega_0(x) = \sqrt{\frac{g.y'(x)}{x}} = \frac{1}{d}\sqrt{gb} \quad (9)$$

The frequency of the isolator is dictated by parameters d and b, as shown in equations (7) and (8), which can be utilized to optimize MVFPI design.

IV. STRUCTURAL MODEL

A three-dimensional single-story building plan resting on the MVFPI is shown in figure 3(a). The isolator was built between the building's base mass and foundation. A stiff deck slab and column make up the superstructure.

The lateral dimension of the deck slab in the x direction is d, and the lateral dimension in the y direction is b. The rigid deck slab is supported by massless, axially inextensible columns, which are coupled to a rigid base slab.
Because the columns are treated as massless and the column masses are included in the slab mass, the Centre of mass is situated at the centre of the deck slab.
The column stiffness distribution is same along the x-axis, on the other hand not along the y-axis. As a result, when excited in the lateral y-direction, the building shows a torsional action. Between the foundation and the stiff base slab are MVFPI isolators. These isolators are attached to the bottom of the foundation and the top of the base slab.
When a structure is subjected to earthquake excitation, its dynamic behaviour is defined by the following degree of freedom: At the centre of the deck slab relative to the base slab, two translational (u_{dx} and u_{dy}) and one rotational ($u_{d\theta}$) degrees of freedom are measured. At the centre of the base slab relative to the ground, two translational, (u_{bx} and u_{by}), and one rotational, ($u_{b\theta}$) degrees of freedom are measured, as well as two isolator's displacement x_b in the x-direction and y_b in the y-direction.
Let k_{xj} and k_{yj} denote the lateral stiffnesses of the jth column in both x- and y-directions, respectively. They are the lateral rigidity of fix base system in x- and y-directions.

$$Kx = \sum_j k_{xj} \quad \text{and} \quad Ky = \sum_j k_{yj} \quad (10)$$

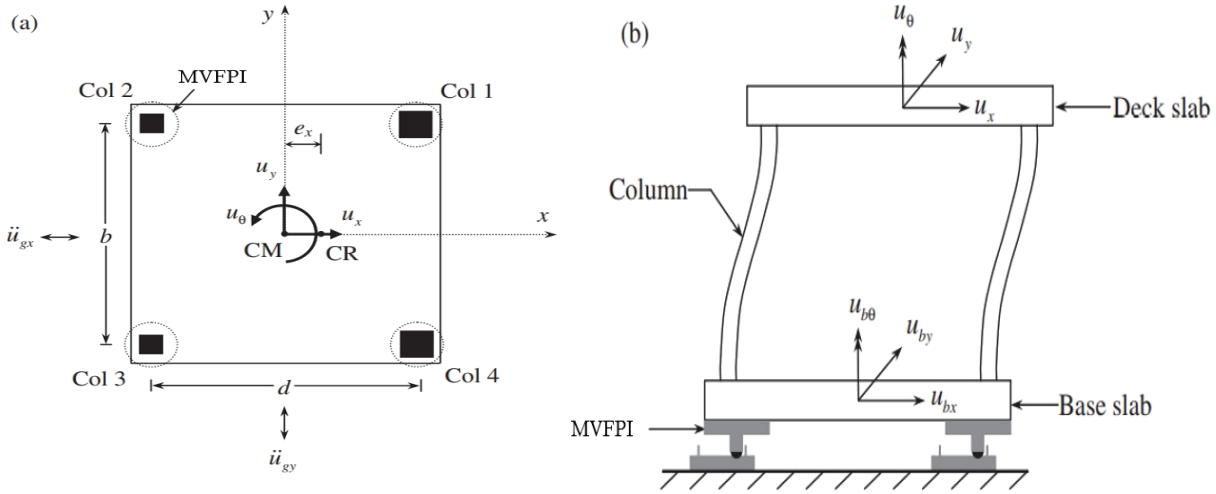

Figure 3. Structural model for MVFPI (A) Plan, (B) Elevation

IARJSET ISSN (O) 2393-8021, ISSN (P) 2394-1588

International Advanced Research Journal in Science, Engineering and Technology

ISO 3297:2007 Certified ⁜ Impact Factor 7.105 ⁜ Vol. 9, Issue 5, May 2022

DOI: 10.17148/IARJSET.2022.9591

Let Xj and Yj denote the jth column's x- and y-coordinates with respect to the centre of mass of the deck slab.

$$K_\Theta = \sum_j k_{xj} Y_j^2 + k_{yj} X_j^2 \quad (11)$$

The torsional rigidity of each column is insignificant and not taken into account. The eccentricity between the deck slab's centre of mass (CM) and the columns' static centre of resistance (CR) is given as,

$$ex = \frac{1}{K_y} \sum_j k_{yj} X_j \quad (12)$$

Corresponding to the translational and rotational modes. The superstructure's three uncoupled modal frequencies will be equal to

$$\omega_x = \sqrt{\frac{K_x}{m_d}}; \qquad \omega_y = \sqrt{\frac{K_Y}{m_d}}; \quad \omega\Theta = \sqrt{\frac{K_\Theta}{m_d r_d^2}}; \quad (13)$$

r_d is the radius of gyration of the deck slab about the vertical axis through the centre of mass, and m is the mass of the superstructure (CM).

Where ωx, ωy and $\omega\theta$ are the normal frequencies of the fixed-base system for torsionally separated, while eccentricity ex = 0, and m, K_x, K_y, and K_Θ are the same as in the coupled system. The deck's torsional mass and the base mass differ, resulting in differently uncoupled torsional to lateral frequency ratios. This can be accomplished by shifting the lumped mass's position relative to the centre of mass (CM).

Let k_{bj} represent the stiffness of the jth MVFPI isolator. Then, in the lateral direction, the isolator's total stiffness, K_b, is given as

$$K_b = \sum_j k_{bj} \quad (14)$$

Where k_{bj} is the same stiffness in both x- and y-directions.

The torsional stiffness of the isolator system is described around the base slab's centre of mass (CM) by,

$$K_{b\Theta} = \sum_j (k_{bj} Y_{jb}^2 + k_{bj} X_{jb}^2) \quad (15)$$

The x- and y-coordinates of the jth MVFPI isolator are denoted by X_{jb} and Y_{jb}, respectively, and the torsional stiffness of each bearing is considered to be modest and ignored.

The jth MVFPI isolator's resultant displacement is computed as,

$$z_{bj} = \sqrt{x_{bj}^2 + y_{bj}^2} \quad (16)$$

$$x_{bj} = u_{bx} - y_{jb} u_{b\Theta} \quad (17)$$

$$y_{bj} = u_{by} - x_{jb} u_{b\Theta} \quad (18)$$

The displacements at the base slab are u_{bx}, u_{by}, and $u_{b\theta}$.

The following are two uncoupled base isolation frequencies,

$$\omega_b = \sqrt{\frac{K_b}{M}} \quad \text{and} \quad \omega_{b\Theta} = \sqrt{\frac{K_{b\Theta}}{mr^2 + m_b r_b^2}} \quad (19)$$

The radius of gyration of the base about the vertical axis through the CM is given by r_b. The stiffness properties of the isolation device are described by the values of ω_b and $\omega_{b\theta}$.

V. GOVERNING EQUATIONS OF MOTION

$$[M]\{\ddot{u}\} + [C]\{\dot{u}\} + [K]\{u\} = -[M][r]\{\ddot{u}b + \ddot{u}g\} \quad (20)$$

$$[Mb]\{\ddot{u}b\} + [Kb]\{ub\} + \{Fb\} - [C]\{\dot{u}\} - [K]\{u\} = -[Mb][r]\{\ddot{u}g\} \quad (21)$$

The lumped mass, stiffness, and damping matrices corresponding to the degree of freedom at the deck are [M], [K], and [C], respectively.

$[u] = \{u_x, u_y, u_\theta\}^T$ is the vector of displacement at the deck relative to the base mass;

$[Mb]$ is the lumped mass matrix corresponding to the degree of freedom at the base mass;

$[Kb]$ is the stiffness matrix of the isolator;

$[Fb] = \{F_x, F_y, F_\theta\}^T$ is the vector of frictional force about the vertical axis;

$[ub] = \{u_x, u_y, u_\theta\}^T$ is the vector of displacement at the base mass;

$[\ddot{u}g] = \{\ddot{u}gx, \ddot{u}gy\}$ is the vector of ground accelerations, $\ddot{u}gx$ and $\ddot{u}gy$ are the ground accelerations in the x- and y-directions, respectively;

IARJSET ISSN (O) 2393-8021, ISSN (P) 2394-1588

International Advanced Research Journal in Science, Engineering and Technology

ISO 3297:2007 Certified ⁜ Impact Factor 7.105 ⁜ Vol. 9, Issue 5, May 2022

DOI: 10.17148/IARJSET.2022.9591

$[r]$ is the earthquake influence coefficient matrix.
The damping matrix [c] isn't specified explicitly. It's made up of the fixed-base structure's anticipated modal dampening and its mode shapes and frequencies. If is the ground acceleration wave's angle of incidence with respect to the x-axis, then the matrix [r] is

$$[\mathrm{r}] = \begin{bmatrix} cos\alpha & -sin\alpha \\ sin\alpha & cos\alpha \\ 0 & 0 \end{bmatrix} \quad (22)$$

The stiffness matrices $[K]$ and $[K_b]$ are written as,

$$[K] = \sum [T_j]^T [k_j] [T_j] \quad (23)$$

$$[k_j] = diag\ [k_{xj}, k_{yj}] \quad (24)$$

$$[\mathrm{T_j}] = \begin{bmatrix} 1 & 0 & -y_j \\ 0 & 1 & x_j \end{bmatrix} \quad (25)$$

$$[\mathrm{K_b}] = \sum [T_{bj}]^T [kj] [T_{bj}] \quad (26)$$

$$[k_{jt}] = diag\ [k_{bj}, k_{bj}] \quad (27)$$

$$[\mathrm{T_{bj}}] = \begin{bmatrix} 1 & 0 & -y_{jb} \\ 0 & 1 & x_{jb} \end{bmatrix} \quad (28)$$

The transformation matrices of the jth column and the MVFPI isolator, respectively, are $[\mathrm{T_j}]$ and $[\mathrm{T_{bj}}]$.
Newmark's step-by-step method is used to solve differential equations of movements (24) and (25) by assuming a linear variation in acceleration over a small time interval, Δt.
For selected approach, the period intermission of 1×10^{-5} has been found appropriate for solving the equations of motion.

VI. PARAMETRIC STUDY

For the following parameters, the reaction of a torsionally coupled structure isolated with the MVFPI to near-fault ground motions is investigated: The superstructure's eccentricity ratio (ex/d), the ratio of uncoupled torsional to lateral frequencies (ω_θ/ω_x), the uncoupled fundamental period of the superstructure (T_x), and the mass ratio (m_b/m_d) are all factors to consider. These factors have an impact on torsional coupling and base isolation characteristics; the range of these parameters was carefully chosen to better understand the impact of system parameters on torsional coupling. . The specifications for the values of the other parameters of structure is given as: The lateral dimension, b = d = 10 m; the number of the MVFPI isolators is 4; modal damping for the superstructure is taken as 2 percent of the critical damping for all modes; and the ratio of the mass of slider to the mass of base slab, (m_s/m_b) is taken as 0.001, Eccentricity in X direction (ex) = 1.5 m, Initial time period of isolator (Tb) = 2.0 sec, Coefficient of friction of isolator (μ)= 0.005, Fix base uncoupled time period (T_x) =1 Sec, Mass ratio floor to base (m_b/m_d) = 1

The current analysis takes into account six response quantities: peak deck slab rotation (u_θ), peak base slab rotation ($u_{b\theta}$), peak base torque, peak resultant isolator displacement (u_{br}), peak base shear in the y-direction, and deck corner displacement magnification. The extent of deformation caused by the combined effects of translation and torsion is represented by the deck corner displacement. The effect of torsional coupling can be determined qualitatively by comparing the level of magnification of deck corner displacement to the displacement at the deck's centre of mass. Corner displacement magnification is employed for this purpose. The ratio of peak deck corner displacement (relative to base) to peak displacement at the CM is what this term refers to (relative to base). The dynamic behaviour of torsionally coupled structures isolated with MVFPI was studied using six sets of near-fault ground motions. Imperial Valley (1979), Array #5, has also been the subject of a comparative investigation of structure isolated with MVFPI and FPS.

IARJSET ISSN (O) 2393-8021, ISSN (P) 2394-1588

International Advanced Research Journal in Science, Engineering and Technology

ISO 3297:2007 Certified ⁜ Impact Factor 7.105 ⁜ Vol. 9, Issue 5, May 2022

DOI: 10.17148/IARJSET.2022.9591

TABLE I CHARACTERISTICS OF THE SELECTED SIX NEAR-FAULT GROUND MOTIONS.

Near-fault Earthquake motions	Recording station	Duration (sec)	Normal component			Parallel component		
			PGD (cm)	PGV (cm/sec)	PGA (g)	PGD (cm)	PGV (cm/sec)	PGA (g)
October 15, 1979 Imperial Valley, California	El Centro Array #5	39.420	76.5	98	0.37	150	52.5	0.55
October 15, 1979 Imperial Valley, California	El Centro Array #7	36.900	49.1	113	0.46	218	55.2	0.34
January 17, 1994 Northridge, California	Newhall	60.000	38.1	119	0.72	17.6	49.3	0.65
June 28, 1992 Landers, California	Lucerne Valley	49.284	230	136	0.71	184	70.3	0.80
January 17, 1994 Northridge, California	Rinaldi	14.950	39.1	175	0.89	18.4	60.2	0.39
January 17, 1994 Northridge, California	Sylmar	60.000	31.1	122	0.73	9.03	53.9	0.6

PGD=Peak Ground Displacement, PGV= Peak Ground Velocity, PGA= Peak Ground Acceleration

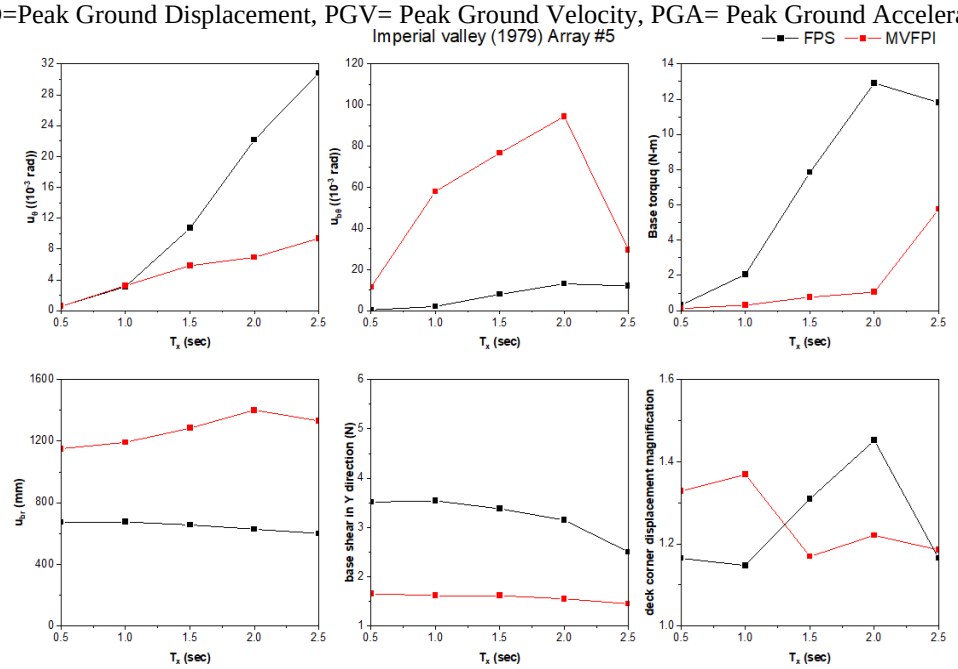

Figure 4. Effect of Tx on the response of the torsionally coupled structure isolated with MVFPI and FPS; $\omega_\Theta/\omega_x = 1.0$, ex/d =0.15, mb/md = 1.0, μ=0.05, d=0.3

A. Comparative Study for Structure Isolated with MVFPI and FPS

Comparative study for torsionally coupled structure isolated with MVFPI and FPS for earthquake ground motion Imperial Valley (1979) Array #5 is illustrated in Figure 4 and 5. It show the torsional lateral peak response of a structure plotted by altering the superstructure's uncoupled fundamental periods (Tx) and the influence of superstructure eccentricity (ex/d) while keeping all other parameters constant. Figure 4. Shows that as the uncoupled fundamental period of the superstructure increases, so does the superstructure's lateral flexibility. As a result, the lateral reaction has little effect,

IARJSET ISSN (O) 2393-8021, ISSN (P) 2394-1588

International Advanced Research Journal in Science, Engineering and Technology

ISO 3297:2007 Certified ⁜ Impact Factor 7.105 ⁜ Vol. 9, Issue 5, May 2022

DOI: 10.17148/IARJSET.2022.9591

whereas the torsional responses increases. As the eccentricity of the superstructure grows in figure 5, the structure's torsional reaction increases. Structures isolated with MVFPI have substantially lower base shear and base torque responses than those isolated with FPS and base rotational displacement. In comparison to the FPS system, the MVFPI system's base displacement is higher.

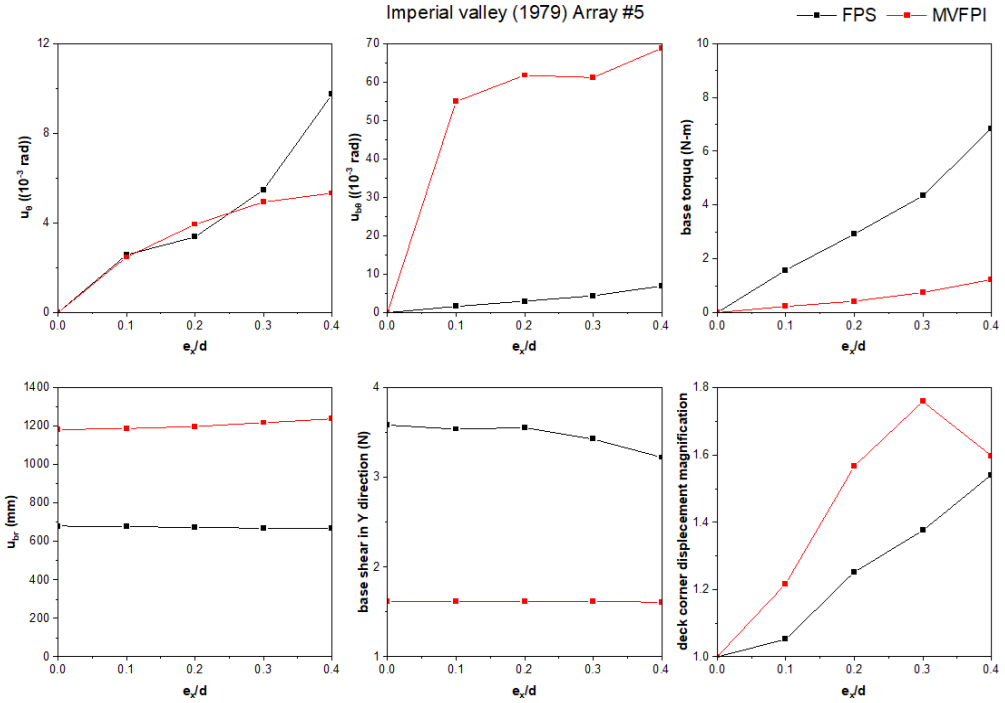

Figure 5. Effect of ex/d on the response of the torsionally coupled structure isolated with MVFPI and FPS; $\omega_\theta/\omega_x = 1.0$, T$x$=2 sec, mb/md = 1.0, μ=0.05, d=0.3

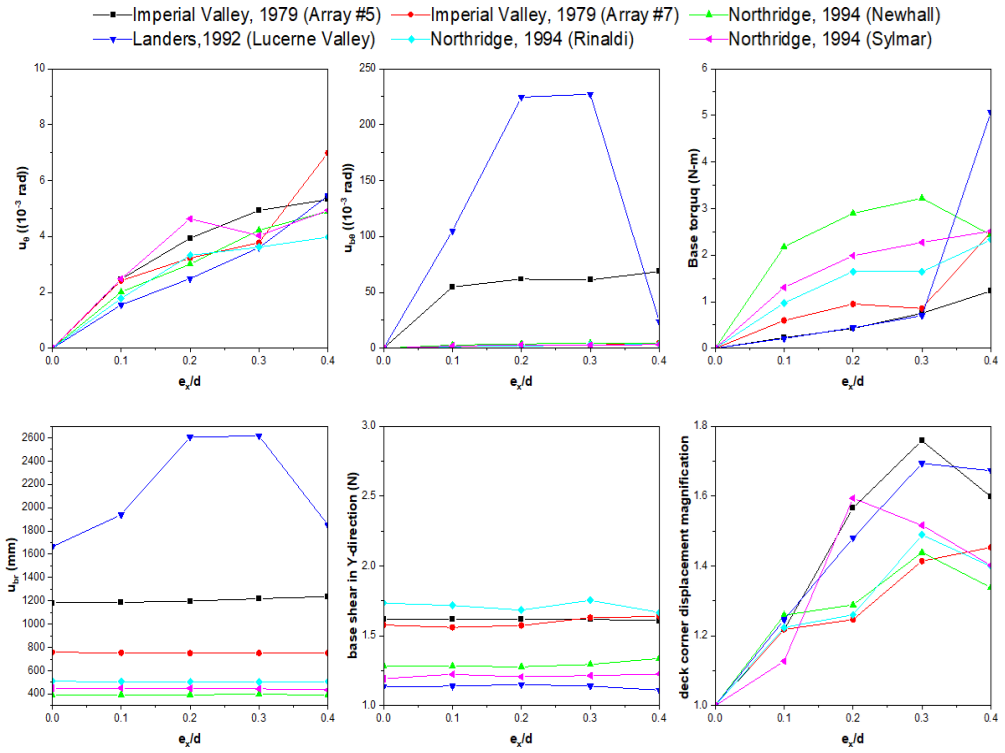

Figure 6. Effect of ex/d on the response of the torsionally coupled structure isolated with MVFPI; $\omega_\theta/\omega_x = 1.0$, T$x$=1.0 sec, mb/md = 1.0, μ=0.05, d=0.3

IARJSET ISSN (O) 2393-8021, ISSN (P) 2394-1588

International Advanced Research Journal in Science, Engineering and Technology

ISO 3297:2007 Certified ⁜ Impact Factor 7.105 ⁜ Vol. 9, Issue 5, May 2022

DOI: 10.17148/IARJSET.2022.9591

B. Effect of Superstructure Eccentricity

The eccentricity of the superstructure (ex/d) is a critical characteristic that causes torsional coupling and torsional motions in structures. Figure 6 depicts the influence of superstructure eccentricity on a torsionally coupled structure isolated with MVFPI (T = 1.0 sec, = 0.05, d = 0.3 m, and b = 0.09) under six different near-fault ground motions. The symmetric scenario (ex/d) = 0 is used in the study, while the asymmetric case (ex/d) = 0.4 is used in the experiment. As shown in Figure 6, torsional reactions, such as deck slab rotation, base slab rotation, and base torque, increase as superstructure eccentricity increases. Superstructure eccentricity has little effect on the lateral response, which includes isolator displacement and peak base shear. With increasing eccentricity, the magnification of deck corner displacement rises.

C. Effect of Torsional to Lateral Frequency Ratio of the Superstructure

The ratio of uncoupled torsional frequency to uncoupled lateral frequency is important in the behaviour of torsionally coupled buildings. Figure 7 shows how increasing ω_θ/ω_x for a certain value causes the deck slab rotation and deck corner magnification ratio to increase, then drop. The base torque and base slab rotation decrease with increases of $\omega\theta/\omega x$, and lateral response remain constant with the variation of ω_θ/ω_x. Thus, the ex/d and ω_θ/ω_x have opposing effects on the coupled lateral-torsional response.

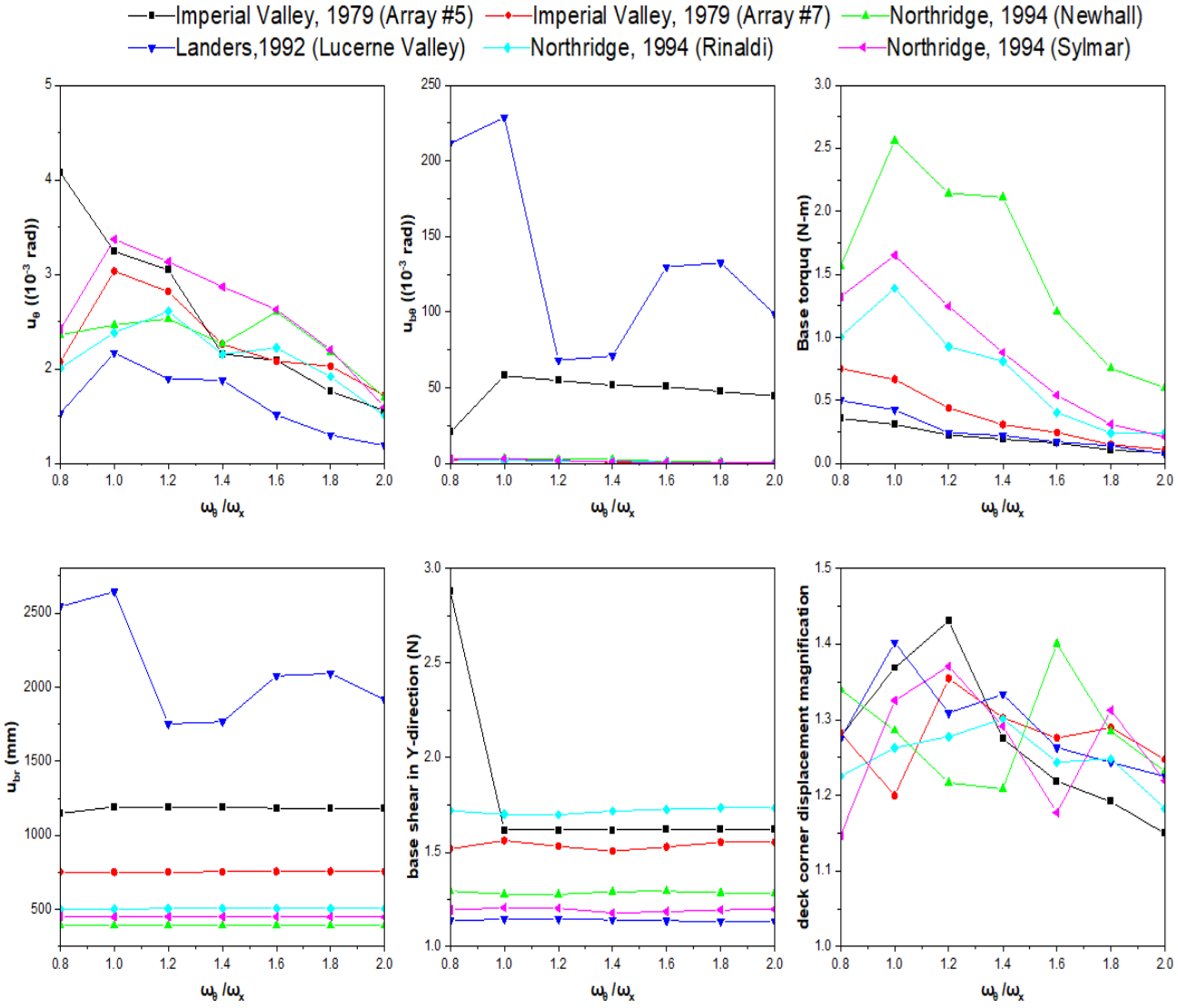

Figure 7. Effect of ω_θ/ω_x on the response of the torsionally coupled structure isolated with MVFPI; ex/d = 0.15, Tx=1.0 sec, mb/md = 1.0, μ=0.05, d=0.3

IARJSET ISSN (O) 2393-8021, ISSN (P) 2394-1588

International Advanced Research Journal in Science, Engineering and Technology

ISO 3297:2007 Certified ⁜ Impact Factor 7.105 ⁜ Vol. 9, Issue 5, May 2022

DOI: 10.17148/IARJSET.2022.9591

D. Fundamental Period of the Superstructure

Figure 8 shows the influence of the uncoupled fundamental period of a superstructure isolated with MVFPI for various Tx values. As the basic period Tx grows, so does the flexibility of the superstructure in the lateral direction, which has no effect on lateral responses but increases all torsional responses. Due to increased lateral displacement of the deck, the deck corner magnification ratio initially surges and then decreases.

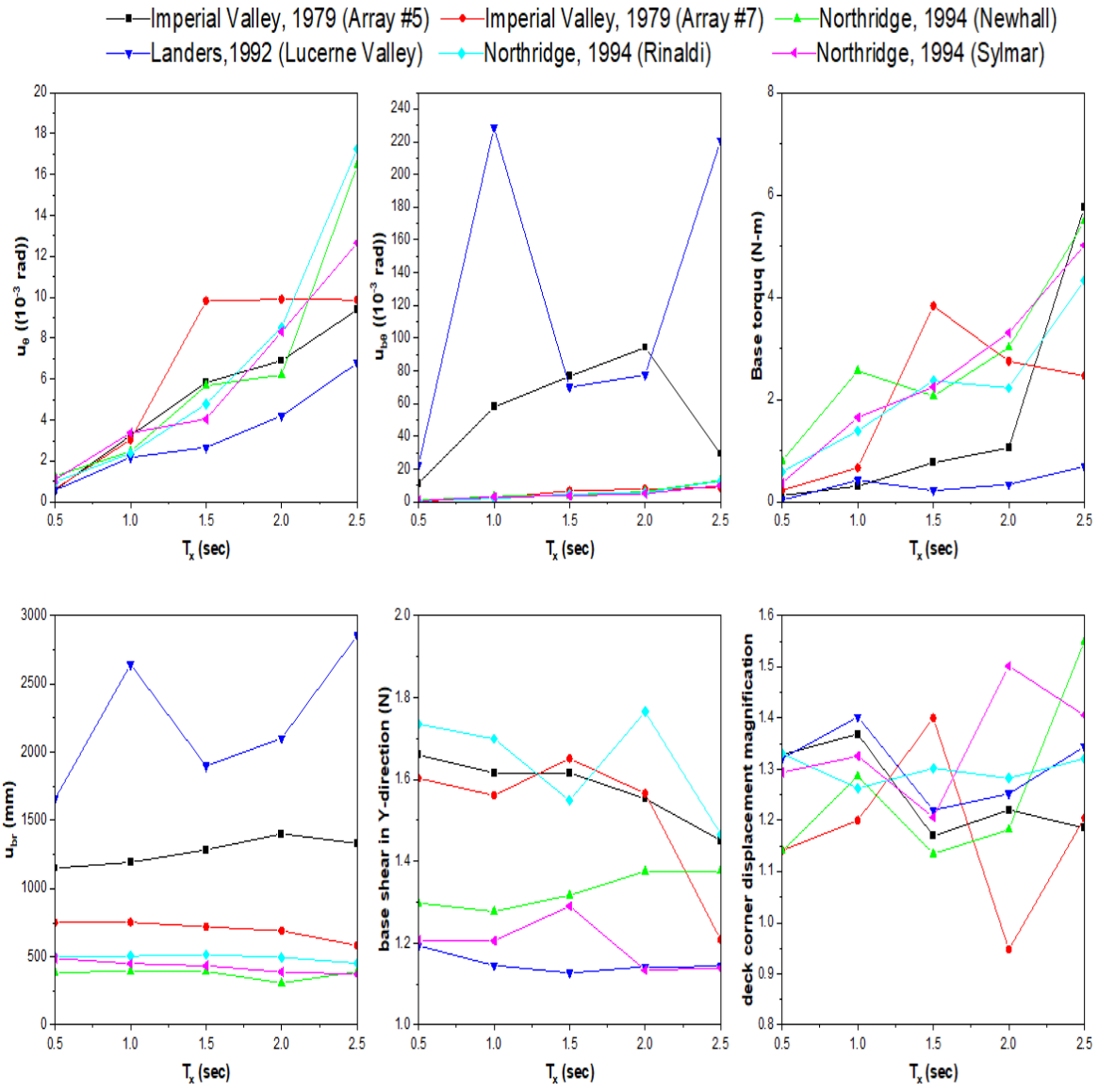

Figure 8. Effect of Tx on the response of the torsionally coupled structure isolated with MVFPI; ex/d = 0.15, $\omega_\theta/\omega_x = 1.0$, mb/md = 1.0, μ=0.05, d=0.3

E. Effect of Mass Ratio

Figure 9 shows the effect of the base to deck mass ratio on torsionally coupled structures isolated with MVFPI. The base shear is heavily influenced by the *mb*/*md* variation. Because it is directly proportional to the weight of the building, the base shear is increasing. With an increase in mass ratio, the base torque and deck slab rotation rise slowly. For all mass ratio values, however, the base rotation, deck corner displacement magnification, and the resulting isolator displacement are nearly identical.

IARJSET ISSN (O) 2393-8021, ISSN (P) 2394-1588

International Advanced Research Journal in Science, Engineering and Technology

ISO 3297:2007 Certified ⁜ Impact Factor 7.105 ⁜ Vol. 9, Issue 5, May 2022

DOI: 10.17148/IARJSET.2022.9591

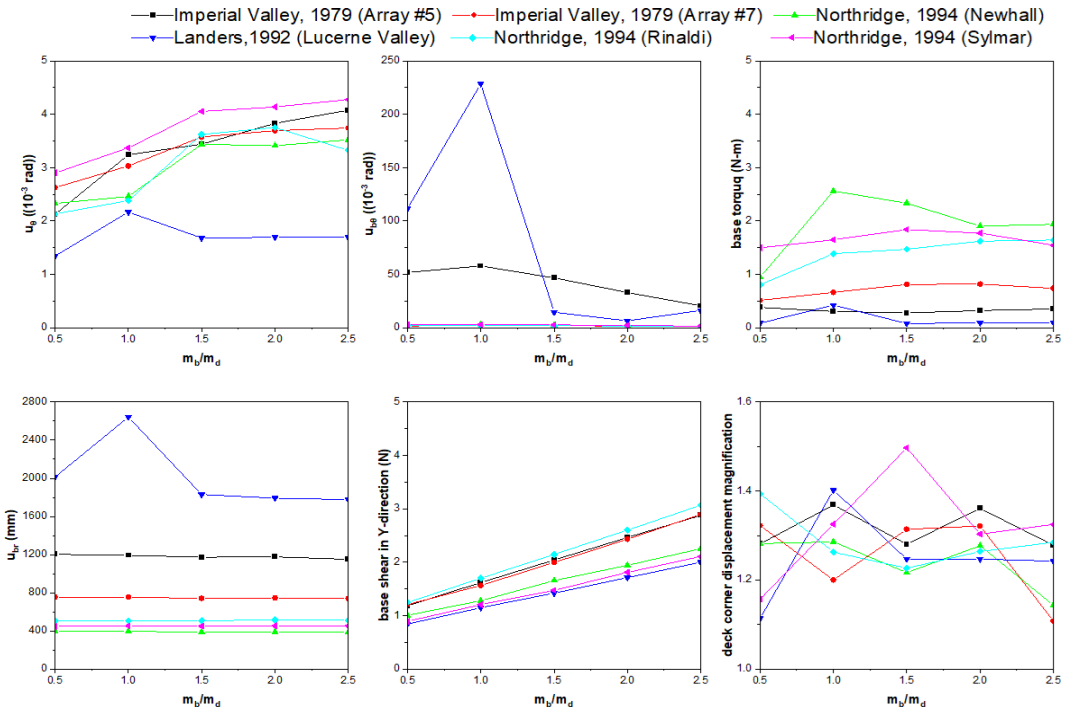

Figure 9. Effect of mb/md on the response of the torsionally coupled structure isolated with MVFPI; ex/d = 0.15, $\omega_\theta/\omega_x = 1.0$, T$x$ = 1.0, μ=0.05, d=0.3

F. Effect of Angle of Incidence

Figure 10 shows variation of structural response is plotted against the angle of incidence (α) for six near-fault ground motions. For some earthquakes, base shear increases and other responses are moderately influenced by the angle of incidence of ground acceleration with respect to the principal direction of the structure.

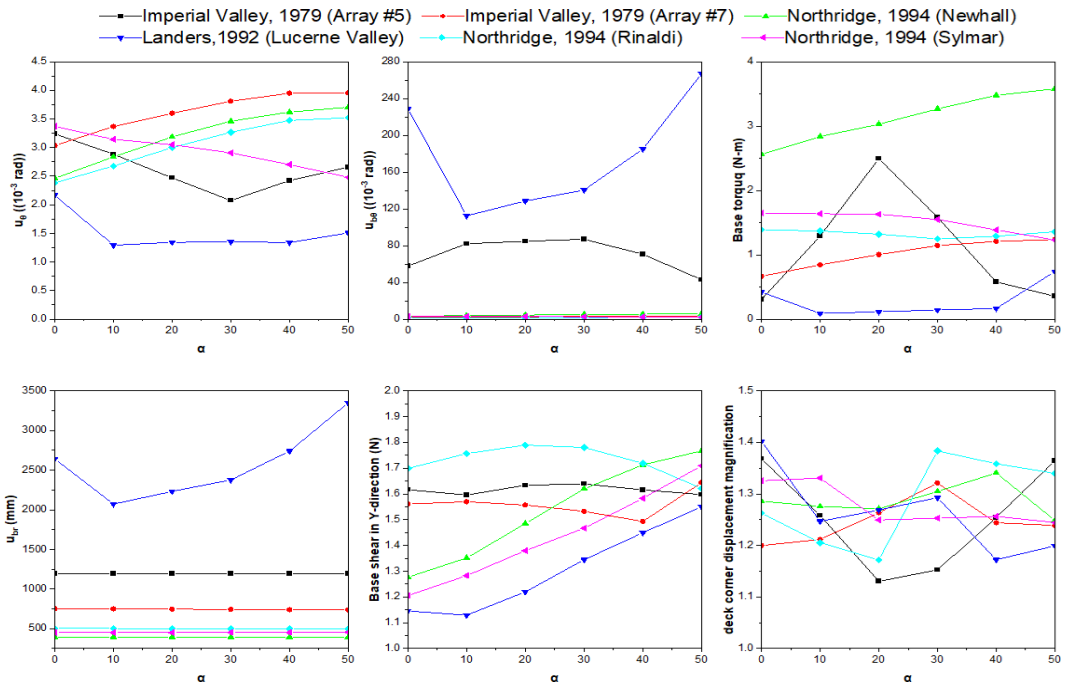

Figure 10. Effect of α on the response of the torsionally coupled structure isolated with MVFPI; ex/d = 0.15, ω_θ/ω_x= 1.0, mb/md=1.0, Tx = 1.0, μ=0.05, d=0.3

IARJSET

International Advanced Research Journal in Science, Engineering and Technology

ISO 3297:2007 Certified ⁜ Impact Factor 7.105 ⁜ Vol. 9, Issue 5, May 2022

DOI: 10.17148/IARJSET.2022.9591

G. Effect of mass Ratio for Rectangular model

Figure 11 shows the effect of the base to deck mass ratio on torsionally coupled structures isolated with MVFPI. The base shear is heavily influenced by the mb/md variation. Because it is directly proportional to the weight of the building, thus the base shear is increasing. Further, with an increase in mass ratio, the deck slab rotation and base torque rises heavily and with compared to square model it got increased by 63% and 136%.

Compared to square model, rectangular model shows decrease in value of deck corner displacement magnification by almost 19%. For all mass ratio values, however, the base rotation and the resulting isolator displacement are nearly identical to square model.

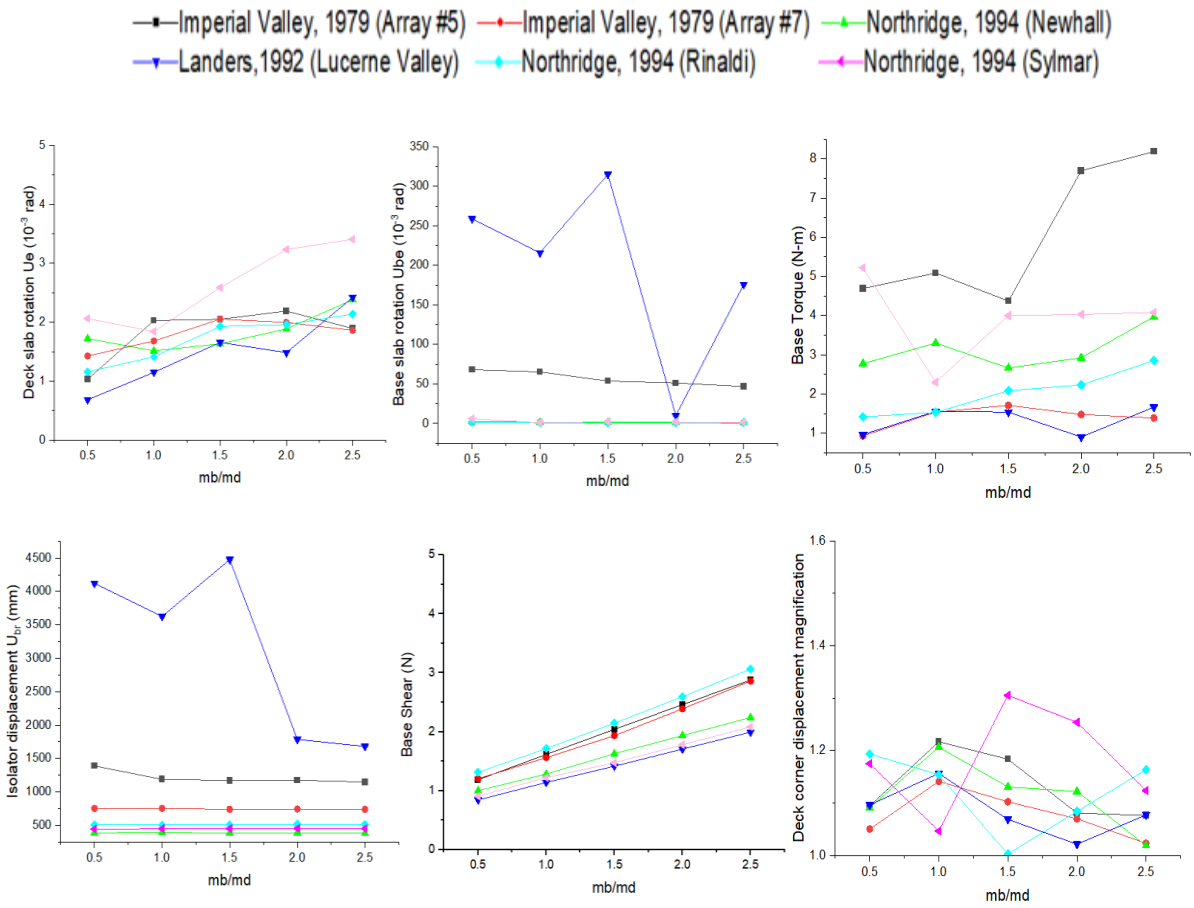

Figure 11. Effect of mb/md on the response of the torsionally coupled structure isolated with MVFPI; ex/d = 0.15, ω_θ/ω_x = 1.0, Tx = 1.0, μ=0.05, d=0.3

VII. CONCLUSION

In two orthogonal directions, the non-linear response of a torsionally coupled system isolated with multiple variable frequency pendulum system (MVFPI) to bilateral near-fault ground motions is measured. Variation of crucial parameters is used to investigate the response behaviour of the torsionally coupled system. The following conclusions can be drawn from this research:

- The geometry of isolators shows that MVFPI's vertical displacement is substantially smaller than FPS's for the same variation of horizontal displacement, resulting in a reduced overturning moment in the MVFPI isolated superstructure.
- e_x/d and ω_θ/ω_x have opposing effects on structural response, according to the research. The torsional response of an asymmetric structure grows as the eccentricity of the superstructure increases. The torsional to lateral frequency ratio exhibits the opposite behavior. The torsional reactivity of the structure rapidly increases as the superstructure eccentricity increases. It suppresses a structure's torsional response as compared to the uncoupled torsional to lateral frequency ratio. As a result, controlling eccentricity rather than increasing superstructure flexibility is preferable.
- The MVFPI system's superstructure flexibility improves torsional response while reducing lateral reactions and deck corner displacement magnification.

IARJSET

International Advanced Research Journal in Science, Engineering and Technology

ISO 3297:2007 Certified ⁜ Impact Factor 7.105 ⁜ Vol. 9, Issue 5, May 2022

DOI: 10.17148/IARJSET.2022.9591

- The ratio of base mass to deck mass has little effect on torsional reactions. The mass ratio, on the other hand, raises base shear dramatically
- The angle of incidence of ground motions with regards to the structure's main axis has a moderate impact on the MVFPI system's Performance.
- When comparing structures with MVFPI to structures with FPS, the value of base shear and base torque is reduced by approximately 90% and 118%, respectively. While MVFPI systems have a higher base rotational displacement and consequent displacement than FPS systems, the asymmetric structure of MVFPI appears to be more effective than FPS.
- Compared to square model, Rectangular model showed increase in value of the deck slab rotation and base torque by 63% and 136% respectively. While decrease in value of deck corner displacement magnification by 19% and rest all other parameters were found to be equal.

REFERENCES

[1]. Zayas VA, Low SS and Mahin SA (1990), "A simple pendulum technique for achieving seismic isolation" Earthquake Spectra, 6: 317–333.
[2]. Murnal, P., & Sinha, R. (2004). Behavior of Torsionally Coupled Structures with Variable Frequency Pendulum Isolator. Journal of Structural Engineering, 130(7), 1041–1054. https://doi.org/10.1061/(asce)0733-9445(2004)130:7(1041)
[3]. Fenz, D.M. and Constantinou, M.C. (2006), "Behaviour of the double concave friction pendulum bearing" Earthq. Eng. Struct. Dyn. 35(11), 1403- 1424.
[4]. Fenz DM and Constantinou MC (2008), "Spherical sliding isolation bearings with adaptive behavior: theory," Earthquake Engineering, and Structural Dynamics, 37: 163–183.
[5]. Tsai CS, Chiang T-C, Chen B-J. (2003), "Finite element formulations and theoretical study for variable curvature friction pendulum system" Engineering Structures; 25(14), 1719–1730.https://doi.org/10.1016/S0141-0296 (03)00151-2
[6]. Pranesh M and Sinha R (2000), "VFPI: an isolation device for aseismic design" Earthq. Eng. Struct.D, 9(5), 603–627. https://doi.org/10.1016/j.nucengdes.2004.03.009
[7]. Murnal, P., & Sinha, R. (2004). Aseismic design of structure-equipment systems using variable frequency pendulum isolator. Nuclear Engineering and Design, 231(2), 129–139. https://doi.org/10.1016/j.nucengdes.2004.03.009
[8]. Panchal V R and Jangid R S (2008), "Variable friction pendulum system forNear-fault ground motions" Struct. Control Health, 15: 568–8.
[9]. Han Q., Liang X., Wen J., Zhang J., Du X. & Wang Z. (2020), "Multiple-variable frequency pendulum isolator with high-performance materials" Smart Materials and Structures, 29(7).
[10]. Hall JF, Heaton TH, Halling M and Wald DJ (1995), "Near-source ground motion and its effects on flexible buildings" Earthquake Spectra, 11: 569– 605.
[11]. Nagarajalah S, Feng MQ and Shinozuka M (1993a), "Control of structures with friction controllable sliding isolation bearings" Soil Dynamics and Earthquake Engineering 12: 103–112.
[12]. Panchal, V. R., & Jangid, R. S. (2012). "Performance of variable friction pendulum system for torsionally coupled structures" JVC/Journal of Vibration and Control, 18(3), 323–343. https://doi.org/10.1177/1077546311407536
[13]. Soni, D. P., Mistry, B. B., & Panchal, V. R. (2010). Behaviour of asymmetric building with double variable frequency pendulum isolator. Structural Engineering and Mechanics, 34(1), 61–84. https://doi.org/10.12989/sem.2010.34.1.061
[14]. Murnal, P. and Sinha, R. (2002), "Earthquake Resistant Design of Structures using the Variable Frequency Pendulum Isolator". Journal of Structural Engineering, 128(7), 870–880. https://doi.org/10.1061/(asce)0733-9445(2002)128:7(870)
[15]. DYNAMICS OF STRUCTURES Theory and Application to Earthquake Engineering by A.K CHOPRA, Fourth Edition, Pearson, ISBN 13: 978-0-13-285803-8
[16]. Reinforced concrete design of tall building by B.S.Taranath, Taylor and francis group, 2014.

